Alleviation of feedback inhibition in Saccharomyces cerevisiae aromatic amino acid biosynthesis: Quantification of metabolic impact

Luttik, M.A.H.; Vuralhan, Z.; Suir, E.; Braus, G.H. ; Pronk, J.T.; Daran, J.G.

DOI
10.1016/j.ymben.2008.02.002

Publication date
2008

Document Version
Final published version

Published in
Metabolic Engineering

Available online at www.sciencedirect.com
ScienceDirect
Metabolic Engineering 10 (2008) 141–153
METABOLIC ENGINEERING
www.elsevier.com/locate/ymben

Alleviation of feedback inhibition in *Saccharomyces cerevisiae* aromatic amino acid biosynthesis: Quantification of metabolic impact

M.A.H. Luttik[a,b], Z. Vuralhan[a,b], E. Suir[a,b], G.H. Braus[c], J.T. Pronk[a,b], J.M. Daran[a,b,*]

[a]*Department of Biotechnology, Delft University of Technology, Julianalaan 67, 2628 BC Delft, The Netherlands*
[b]*Kluyver Centre for Genomics of Industrial Fermentations, Julianalaan 67, 2628 BC Delft, The Netherlands*
[c]*Department of Molecular Microbiology and Genetics, Georg-August University, Grisebachstr. 8. 37077 Göttingen, Germany*

Received 14 November 2007; received in revised form 2 February 2008; accepted 5 February 2008
Available online 20 February 2008

Abstract

A quantitative analysis of the impact of feedback inhibition on aromatic amino acid biosynthesis was performed in chemostat cultures of *Saccharomyces cerevisiae*. Introduction of a tyrosine-insensitive allele of *ARO4* (encoding 3-deoxy-D-*arabino*-heptulosonate-7-phosphate synthase) caused a three-fold increase of intracellular phenylalanine and tyrosine concentrations. These amino acids were not detected extracellularly. However, an over 100-fold increase of the extracellular levels of phenylacetate, phenylethanol and their para-hydroxyl analogues was observed. The total increase of the flux through the aromatic pathway was estimated to be over four-fold. Individual overexpression of either the wild-type or feedback insensitive allele of *ARO7* (encoding chorismate mutase had no significant impact. However when they were combined with the Tyr-insensitive *ARO4* allele in combination with the Tyr-insensitive *ARO4* allele, extracellular concentrations of aromatic compounds were increased by over 200-fold relative to the reference strain, corresponding to a 4.5-fold increase of the flux through the aromatic amino acid biosynthesis pathway. Elimination of allosteric control on these two key reactions in aromatic amino acid metabolism significantly affected intracellular concentrations of several non-aromatic amino acids. This broader impact of amino acid biosynthesis presents a challenge in rational optimization of the production of specific amino acids and derived flavour compounds.

Keywords: Chemostat culture; *Saccharomyces cerevisiae*; Aromatic amino acid biosynthesis; Chorismate mutase; DAHP synthase; Feedback inhibition

1. Introduction

The aromatic amino acids phenylalanine and tryptophan are mainly used in food and feed applications. They are produced on an industrial scale via bacterial fermentation processes using *Escherichia coli* and *Corynebacterium glutamicum* (Pittard, 1996; Hermann, 2003). Interest in phenylalanine has increased proportionally with the increased demand for low caloric food and soft drinks, as phenylalanine is a precursor for the low caloric sweetener aspartame (Gunby, 1983; Sprenger, 2007). While *Saccharomyces cerevisiae* is not under consideration for the industrial production of amino acids, aromatic amino acid metabolism by this yeast is of interest for other industrial applications.

In *S. cerevisiae* and other yeasts (Fabre et al., 1998; Wittmann et al., 2002) the phenylalanine biosynthesis pathway is involved in the synthesis of phenylethanol. This molecule has interesting sensory properties (including a rose-like aroma) and is of increasing economical interest. Phenylethanol can be produced via bio-transformation of phenylalanine with *S. cerevisiae* (Etschmann et al., 2002). This conversion involves the reactions of the Ehrlich pathway (Ehrlich, 1907), which is involved in the catabolism of several amino acids by *S. cerevisiae* (Fig. 1). In the case of phenylalanine, the Ehrlich pathway is initiated by its transamination to phenylpyruvate. This 2-oxo acid is then decarboxylated to phenylacetaldehyde (Vuralhan

*Corresponding author at: Department of Biotechnology, Delft University of Technology, Julianalaan 67, 2628 BC Delft, The Netherlands.
E-mail addresses: j.m.daran@tudelft.nl, j.g.daran@tudelft.nl (J.M. Daran).

1096-7176/$ - see front matter © 2008 Elsevier Inc. All rights reserved.
doi:10.1016/j.ymben.2008.02.002

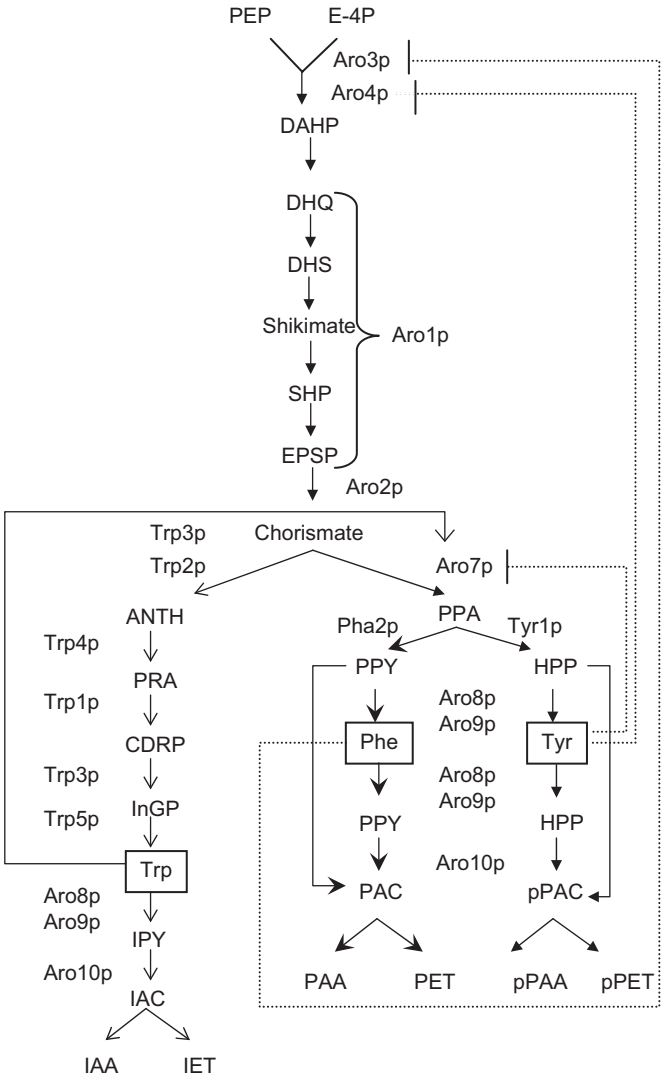

Fig. 1. Pathways of aromatic amino acid biosynthesis and catabolism in *S. cerevisiae*. The dashed lines indicate feedback inhibition of Aro4p and Aro7p by tyrosine and feedback inhibition of Aro3p by phenylalanine. The solid line indicates activation of Aro7p by tryptophan. E-4P: erythrose 4-phosphate, PEP: phosphoenol pyruvate, DAHP: 3-deoxy-D-arabino-heptulosonate-7-phosphate, DHQ: 3-dehydroquinate, DHS: 3-dehydro-shikimate, SHP: shikimate-3-phosphate, EPSP: 5 enolpyruvoylshikimate 3-phosphate, ANTH: anthranilate, PRA:phosphoribosyl anthranilate, CDRP: 1-(o-carboxyphenylamino-1-deoxyribulose 5-phosphate, InGP: indole 3-glycerol-phosphate, PPA: prephenate, PPY: phenylpyruvate, HPP: *para*-hydroxy-phenylpyruvate, PAC: phenylacetaldehyde, PAA: phenylacetate, PET: phenylethanol, *p*PAC: *para*-hydroxy-acetaldehyde *p*PAA:para-hydroxy-acetate, *p*PET: *para*-hydroxy-phenylethanol, IAC: indole-acetaldehyde, IAA: indole-acetate, IET: indole-ethanol, Trp: tryptophan, Phe: phenylalanine, Tyr: tyrosine.

et al., 2005). Depending on the redox status of the cells, phenylacetaldehyde is then reduced by alcohol dehydrogenases (yielding phenylethanol) or oxidized to phenylacetic acid by aldehyde dehydrogenases (Vuralhan et al., 2003). Phenylpyruvate, the precursor for phenylethanol production by *S. cerevisiae*, is also an intermediate in the *de novo* biosynthesis of phenylalanine from sugars.

In bacteria, extensive strain improvement programmes, involving a combination of random mutagenesis and targeted metabolic engineering, have been applied to improve aromatic amino acid biosynthesis (Ikeda and Katsumata, 1992; Ikeda, 2003; Sprenger, 2007; Lütke-Eversloh et al., 2007). In these strain improvement programmes, a first and essential step is invariably the elimination of feedback inhibition on key enzymes in the biosynthetic pathway. In *S. cerevisiae*, two reactions in the phenylalanine biosynthesis pathway are known to be subject to feedback inhibition (Fig. 1). The first committed step in aromatic amino acid metabolism is catalysed by 3-deoxy-D-*arabino*-heptulosonate-7-phosphate (DAHP) synthase, for which two isoenzymes exist in *S. cerevisiae*, encoded by the *ARO3* and *ARO4* genes (Teshiba et al., 1986; Kunzler et al., 1992). Aro3p and Aro4p are feedback inhibited by phenylalanine and tyrosine, respectively. Besides, considerable tryptophan regulation of DAHP synthase has recently been reported (Helmstaedt et al., 2005). A single lysine-to-leucine substitution in Aro4p at position 229 results in a deregulated enzyme that is no longer feedback inhibited by tyrosine (Hartmann et al., 2003). Chorismate mutase, encoded by *ARO7*, has been identified as a second reaction subject to allosteric regulation (Ball et al., 1986; Brown and Dawes, 1990), its activity is inhibited by tyrosine and stimulated by tryptophan. Substitution of the serine residue 141 by a glycine abolished effects of both tyrosine and tryptophan, thus leading to a non-allosterically regulated chorismate mutase (Schnappauf et al., 1998; Krappmann et al., 2000). Although considerable knowledge is available on the molecular basis for feedback inhibition of aromatic amino acid metabolism (Helmstaedt et al., 2001), no quantitative studies have yet been performed on its impact on product formation by growing *S. cerevisiae* cultures.

The aim of this study is to quantify the combinatorial effects of deregulation of DHAP synthase and chorismate synthase in *S. cerevisiae*. To this end, a tyrosine-feedback insensitive DAHP synthase and a non-allosterically regulated chorismate mutase were expressed in an *aro3Δ* genetic background. Subsequently, the production of aromatic amino acids and the corresponding fusel alcohols and 'fusel acids' were quantified in aerobic, glucose-limited chemostat cultures. To assess the specificity of this approach to deregulate aromatic amino acid metabolism, we also analysed intracellular concentrations of other amino acids in reference and engineered strains.

2. Materials and methods

2.1. Strain construction and maintenance

The *S. cerevisiae* strains used in this study are listed in Table 1. Stock cultures were grown at 30 °C in shake flasks on synthetic medium (SM) (Luttik et al., 1998) supplemented with glucose (20 g l^{-1}) (for composition see growth condition section). When stationary phase was reached, sterile glycerol was added to 30% (vol/vol), and 2-ml aliquots were stored in sterile vials at −80 °C.

Table 1
Saccharomyces cerevisiae strains used in this study

Strain	Genotype	Reference
CEN.PK122	MATa/MATα prototrophic reference diploid strain	P. Kötter[a]
CEN.PK113-7D	MATa Prototrophic reference haploid strain, *ARO3 ARO4 ARO7*	P. Kötter[a]
CEN.PK113-5D	MATa *ura3 ARO3 ARO4 ARO7*	P. Kötter[a]
CEN.PK113-13D	MATα *ura3 ARO3 ARO4 ARO7*	P. Kötter[a]
CEN.PK437-1C	MATα *ARO3 aro4Δ*	This study
CEN.PK532-1A	MATa *aro3Δ ARO4*	This study
CEN.PK532-1C	MATα *aro3Δ ARO4*	This study
CEN.PK557-5A	MATa *aro3Δaro4Δ*	This study
CEN.PK621-1B	MATa *TPI1pr-ARO4*	This study
CEN.PK661-1C	MATa *aro3Δ TPI1pr-ARO4*	This study
CEN.PK718-5A	MATa *aro3Δ* $ARO4^{K229L}$	
CEN.PK790-2D	MATa *ura3 aro3Δ* $ARO4^{K229L}$	This study
IMN02	MATa *aro3Δ TDH3pr*::$ARO4^{K229L}$	This study
IMN03	MATa *ura3 aro3Δ TDHpr3*::$ARO4^{K229L}$ pUDe003 *(2μ URA3 TDH3pr-ARO7)*	This study
IMN04	MATa *ura3 aro3Δ TDH3pr*::$ARO4^{K229\ L}$pUDe004*(2μ URA3 TDH3pr-*$ARO7^{G141S}$*)*	This study
IMN05	MATa *ura3 ARO3 TDH3pr*::$ARO4^{K229}$ p426-GPD *(2μ URA3 TDH3pr)*	This study
IMZ014	MATa *ura3 aro3Δ* $ARO4^{K229L}$ *pUDe003 (2μ URA3Δ TDH3pr-ARO7)*	This study
IMZ016	MATa *ura3 ARO3 ARO4 pUDe003 (2μ URA3Δ TDH3pr-ARO7)*	This study
IMZ017	MATa *ura3 ARO3 ARO4 pUDe004 (2μ URA3Δ TDH3pr-* $ARO7^{G141S}$*)*	This study
IMZ018	MATa *ura3 aro3Δ* $ARO4^{K229L}$ *pUDe004 (2μ URA3Δ TDH3pr-ARO7* ^{G141S}*)*	This study

[a]Institüt für Mikrobiologie der J. W. Goethe Universität, Frankfurt, Germany.

The construction of the *ARO3* and *ARO4* null mutants was done using the PCR-based short flanking homologies (SFH) method. SFH deletion cassettes were obtained by PCR using the primers pairs *ARO3*-S1/*ARO3*-S2 and *ARO4*-S1/*ARO4*-S2 (Table S1) with pUG6 as template (Guldener et al., 1996). The deletion cassettes were transformed in the prototrophic diploid yeast strain CEN.PK122. After sporulation and tetrad analysis the corresponding segregants were isolated resulting in strains CEN.PK532-1A and CEN.PK437-1C. Both strains were crossed to obtain after tetrad analysis the *aro3 aro4* double deletion strain CEN.PK557-5A.

The plasmid pME2027 harbouring the $ARO4^{K229L}$ (Hartmann et al., 2003) was PCR-amplified using the primers *ARO4*-A8/*ARO4*-A9 (Table S1) yielding a fragment starting at nucleotide 7 to 1106 of the *ARO4* coding region. The resulting PCR product was transformed in the *aro3Δ aro4Δ* double deletion strain CEN.PK557-5A and transformants were selected on SM plates. Sequencing using primer *ARO4*-A11 (Table S1) proofed the *ARO4* point mutation in the obtained strain CEN.PK718-5A.

The addition of the *ura3-52* allele in the *aro3Δ* $ARO4^{K229L}$ strain CEN.PK718-5A was achieved by crossing it with the strain CEN.PK113-13D (*ura3-52*). After tetrad analysis the corresponding segregants were identified on the respective media (YEPD, YEPD + G418, SCD-ura, SCD + trp + tyr + phe, SCD + trp + tyr, SCD + ura + trp + tyr and SCD + ura + trp + tyr + phe) and the $ARO4^{K229L}$ point mutation of resulting strain CEN.PK790-2D was confirmed again by sequencing using primer *ARO4*-A11. The loxP-KanMX-loxP cassette was removed according to (Guldener et al., 1996). The original *ARO4* promoter in the strain CEN.PK790-2D G418 sensitive was exchanged with a *TDH3* promoter. The PCR fragment carrying the constitutive promoter was amplified using the primer pair ARO4T1/ARO4P2 (Table S1) and the vector pYM-N14 as a template (Janke et al., 2004). Correct integration of the $TDH3_{pr}$-loxP-KanMX-loxP cassette was confirmed by diagnostic PCR. The resulting strain was named IMN02.

To express the *ARO4* gene under the control of the *TPI1* promoter the loxP-KanMX-loxP-$TPI1_{pr}$ cassette was amplified using primers *ARO4*-T1 and *ARO4*-P2 and pPK261 that carries the$TPI1_{pr}$-loxP-KanMX4-loxP integration cassette as template. The resulting PCR product was transformed in the diploid strain CEN.PK122 and transformants were selected on YPD + G418 plates. After sporulation and tetrad analysis the corresponding segregants were isolated resulting in strain CEN.PK621-1B. Correct integration of the $TPI1_{pr}$-loxP-KanMX-loxP cassette was confirmed by diagnostic PCR. For the construction of the *aro3* $TPI1_{pr}$-*ARO4* strain CEN.PK661-1C, the two strains CEN.PK532-1C and CEN.PK621-1B were crossed and segregants were isolated showing in tetrad analysis a 2:2 segregation of the kan^r-marker plasmid.

The *ARO7* wild-type and mutant $ARO7^{G141S}$ open reading frame were PCR-amplified from CEN.PK113-7D genomic DNA and pME1463 plasmid DNA (Schnappauf et al., 1998), respectively, using primers *ARO7*-fwd and *ARO7*-rev (Table S1) designed to introduce restriction sites for endonuclease *Nhe*I, upstream of the ATG and *Xho*I, downstream of the stop codon, respectively. The PCR product and the 2 μm-based expression vector p426GPD (Mumberg et al., 1995) were digested by *Xba*I and *Xho*I.

The *Nhe*I-*Xho*I PCR fragments were directionally cloned behind the glyceraldehyde-3-phosphate dehydrogenase promoter (*TDH3pr*) into p426GPD resulting in plasmids pUDe003 (*ARO7*) and pUDe004 ($ARO7^{G141S}$). The *ARO7* open reading frame sequences were confirmed by sequencing. The plasmids pUDe003 and pUDe004 were transformed by the LiAc/SS/PEG method (Gietz and Schiestl, 2007) into the *S. cerevisiae* CEN.PK113-5D strain resulting in strain IMZ016 and IMZ017, respectively. Similarly, the plasmids pUDe003, pUDe004 and p426-GPD were transformed into the *S. cerevisiae* IMN02 strain resulting in strains IMN03, IMN04 and IMN05, respectively (Table 1).

2.2. Growth conditions

Shake flask cultures were performed as described previously (van Maris et al., 2004). The SM (Luttik et al., 1998) contained 20 g l^{-1} glucose as carbon source and 5 g l^{-1} ammonium sulphate as nitrogen source. Where mentioned, filter-sterilized L-tryptophan was added to a concentration of 50 mg l^{-1}. Growth rate of the various strains represented average and mean deviation of three independent cultivations.

To test growth inhibition by L-tyrosine, 24 h SM-shake flask cultures were streaked out on SM-agar plates with 2% glucose and L-tyrosine concentrations ranging from 0 to 1 mM. After inoculation, the plates were incubated at 30 °C for 52 h.

Steady-state chemostat cultures were grown in Applikon laboratory fermentor of 1-l working volume (Applikon, Schiedam, The Netherlands), as described in detail elsewhere (van den Berg et al., 1996). The cultures were fed with a defined SM containing glucose as the growth-limiting nutrient (Verduyn et al., 1990). The dilution rate (which equals the specific growth rate) in the steady-state cultures was 0.10 h^{-1}, the temperature was 30 °C, and the culture pH was 5.0. Aerobic conditions were maintained by sparging the cultures with air (0.5 l $r\,min^{-1}$). The dissolved oxygen concentration, which was continuously monitored with an Ingold model 34-100-3002 probe (Mettler-Toledo, Greifensee, Switzerland), remained above 50% of air saturation. Two independent chemostat cultures were run for each tested strain.

2.3. Culture dry weight

Culture dry weight was determined via filtration as described previously (Postma et al., 1989).

2.4. Extracellular metabolite analysis

Culture supernatants and media were analysed by high-performance liquid chromatography (HPLC), fitted with an AMINEX HPX-87H ion-exchange column (300 mm × 7.8 mm; Bio-Rad) mounted in a Waters Alliance 2690 HPLC apparatus, at 60 °C using H_2SO_4 as the mobile phase having a flow rate of 0.6 ml min^{-1}. Aromatic amino acid metabolites were analysed by a dual-wavelength absorbance detector (Waters 2487) and integrated with Chrompack Maitre 2.5 software. Each biological sample was measured in triplicates.

2.5. Intracellular metabolite analysis

Thirty millilitre of cell broth was collected at steady state. The cells were spun down at 4 °C, 5000 rpm for 5 min. The pellet was resuspended in 10 ml of boiling water and incubated above 90 °C in a thermo-bath for 10 min. Subsequently, cells were spun down. The supernatant was collected and then evaporated in a Speedvac® under full vacuum conditions. The sample was resuspended in 300 μl of H_2O before further processing. A Phenomenex amino acid kit for GC-MS (Phenomenex Inc., Torrence, CA, USA) was used to measure intracellular amino acid concentrations. The amino acids were derivatized according the supplier's recommendations after a solid phase extraction on a strong cation exchanger to remove proteins and other interfering sample components; the amino group was alkylated with alkyl chloroformate while the carboxylic group was simultaneously esterified. The volatile alkoxycarbonyl alkyl esters of amino acids were injected into a GC-MS TRACE DSQ™ (Dual-Stage Quadrupole) (ThermoFinnigan, San Jose, CA, USA.). The GC temperature programme as proposed by Phenomenex was: initial temp 110 °C, ramped to 320 °C at 30 °C min^{-1} (hold 1 min) with a column flow of 1.1 ml min^{-1}. Each biological sample was measured in triplicates. To compare genotype-dependent concentration profiles for different amino acids, average concentrations were normalized relative to the concentration in the reference strain CEN.PK113-7D:

$$\text{Relative}[AA_j]^{\text{strain } i} = ([AA_j]^{\text{strain } i}/[AA_j]^{\text{CEN.PK113-7D}}) \times 100\%$$

This normalized data set was submitted to hierarchical data clustering and the data presented as a heat map using Genedata® expressionist (Genedata, Basel, Switzerland).

2.6. Enzyme assays

2.6.1. Chorismate mutase

Cell extract was prepared as described previously (Vuralhan et al., 2003) Chorismate mutase (EC 5.4.99.5) was assayed according to Schmidheini et al. (1989) with minor modifications. A 1 ml incubation mix with Tris–HCl pH 7.6 (50 mM), dithiothreitol (DTT, 1 mM), and EDTA (0.1 mM) was incubated with cell extract (20–200 μl) at 30 °C. At $t = 0$ min, 1 mM (final concentration) of barium chorismate was added. In order to check allosteric control of the various alleles of *ARO7* used in this study, either 0.5 mM of tyrosine or 0.5 mM of tryptophan were used to test inhibition or activation, respectively. For the duration of 5 min, a 100-μl sample was taken every minute, and added to 100 μl of 1 M HCl. These samples were incubated

at 30 °C for 10 min, after which 800 µl of 1 M NaOH was added. Absorbance was measured at 320 nm, an experimentally determined (data not shown) extinction coefficient of 13.165 $mM^{-1} cm^{-1}$ was used to calculate the phenylpyruvate concentration. Each cell extract was measured in triplicates.

Blank measurements and controls with prephenic acid or phenylpyruvic acid showed no detectable substrate decay or chemical decay of the product formed. Specific activities were linearly proportional to the amount of cell extract added.

2.6.2. DAHP synthase

Cell extract was prepared as described previously (Vuralhan et al., 2003) except that the FastPrep system (MP Biomedicals, Solon, USA) was used for cell disruption. One millilitre aliquots of cell suspension were pipetted in two cooled safelock Eppendorf tubes each containing 0.75 g of glass beads (425–600 µm, Sigma, St. Louis, USA). After 4 runs of 20 s at speed setting 6 with intermittent cooling, cell extracts were centrifuged as described previously by Vuralhan et al. (2003). Prior to DAHP-synthase assays, metabolites and small molecules were removed from the cell extract using Vivaspin4 (10,000 MWCO) columns (Sartorius Technologies BV, Nieuwegein) according to manufacturers protocol in three runs (30 min at 4000*g*, and at 4 °C). The buffer used for desalting was identical to that for preparation of the cell extract, without the addition of DTT.

The DAHP-synthase assay (modified from Sprinson et al., 1962) was performed as follow: the mixture of 1 ml contained 100 mM KPB buffer, 0.5 mM phophoenolpyruvate (PEP) and 1 mM erythrose-4-phosphate (E-4P). The reaction was started with the addition of cell extract. After 2, 3, 4 and 5 min of reaction time, 200 µl of the reaction mixture was transferred to an Eppendorf tube containing 80 µl of 10% w/v trichloroacetic acid solution. The resulting mixture was centrifuged for 5 min in an Eppendorf table centrifuge to remove proteins. About 125 µl of the supernatants was transfered to clean Eppendorf tubes and 125 µl periodic acid (25 mM in 0.075 M H_2SO_4) was added to each tube. In order to check allosteric control of the various alleles of *ARO4* used in this study, either 0.5 mM of tyrosine, 0.5 mM phenylalanine or 0.5 mM of tryptophan were used to test inhibition. After incubation at room temperature for 45 min 0.25 ml of 2% (w/v) sodium arsenite in 0.5 M HCl was added to destroy excess periodate (2 min at room temperature). One millilitre of thiobarbituric acid (0.3%, w/v, pH 2.0) was added to the tubes, which were subsequently placed in a boiling-water bath for 5 min. The mixture was cooled in a water bath for 10 min at 40 °C and the pink colour developed was measured at 549 nm in a Hitachi U3010 spectrophotometer against air. The extinction coefficient of DAHP at 549 nm was 13.6 $mM^{-1} cm^{-1}$ in the above assay, no decay of absorbance was observed for at least 30 min at 30 °C. Each cell extract was measured in triplicates.

2.7. Protein determination

Protein concentrations in cell extracts were determined by the Lowry method (Lowry et al., 1951). Bovine serum albumin (fatty acid free; Sigma, St. Louis, Mo.) was used as a standard.

3. Results

3.1. Elimination of allosteric control on DAHP synthase and chorismate mutase

To confirm that the expression of the $ARO4^{K229L}$ and $ARO7^{G141S}$ alleles resulted in the elimination of allosteric control on DAHP synthase and chorismate mutase, respectively, plate assays and in vitro enzyme activity measurements were performed. Plate assays in the presence of 1 mM tyrosine completely inhibited growth of *aro3Δ* strain CEN.PK532-1A (Fig. 2), thus confirming the tyrosine-feedback sensitivity of the Aro4p-encoded DAHP synthase in the CEN.PK strain background. This tyrosine sensitivity could not be overcome by overexpression of the wild-type *ARO4* allele (strain CEN.PK666-1C, Fig. 2). However, introduction of the $ARO4^{K229L}$ allele completely

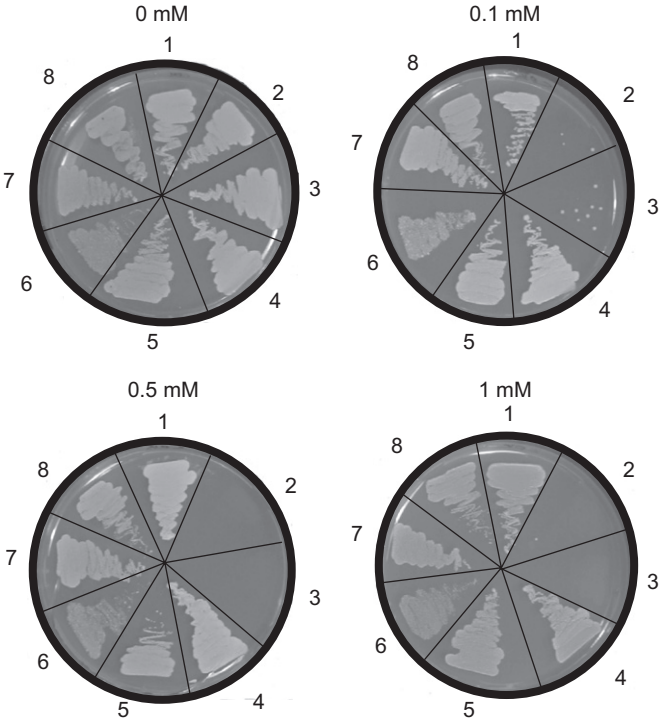

Fig. 2. Growth inhibition by L-tyrosine of the reference *S cerevisiae* strain CEN.PK113-7D and strains engineered in key steps of aromatic amino acid biosynthesis. The yeast strains were streak on SM medium with 2% glucose containing either 0 (left top panel), 0.1 mM (right top panel), 0.5 mM (left bottom panel) or 1 mM (right bottom panel) L-tyrosine. Plates were incubated at 30 °C for 52 h. 1: CEN.PK113-7D (prototrophic reference strain) 2: CEN.PK532-1A (*aro3Δ ARO4*) 3: CEN.PK666-1C (*aro3Δ TPI1p-ARO4*) 4: CEN.PK718-5A ($aro3\Delta\ ARO4^{K229L}$) 5: IMZ014 ($aro3\Delta\ ARO4^{K229L}$ *TDH3-ARO7*) 6: IMZ018 ($aro3\Delta\ ARO4^{K229L}$ *TDH3-*$ARO7^{G141S}$) 7: IMZ016 (*TDH3-ARO7*) 8: IMZ017 (*TDH3-* $ARO7^{G141S}$).

eliminated the tyrosine sensitivity (Fig. 2), thus confirming the lack of tyrosine sensitivity of the DAHP synthase encoded by this mutant allele (Hartmann et al., 2003). Allosteric control of DAHP synthase in the strains used in this study was further analysed by measuring enzyme activities in cell extracts, prepared from glucose-limited chemostat cultures. Although levels of DAHP-synthase activity in cell extracts varied among replicate experiments,

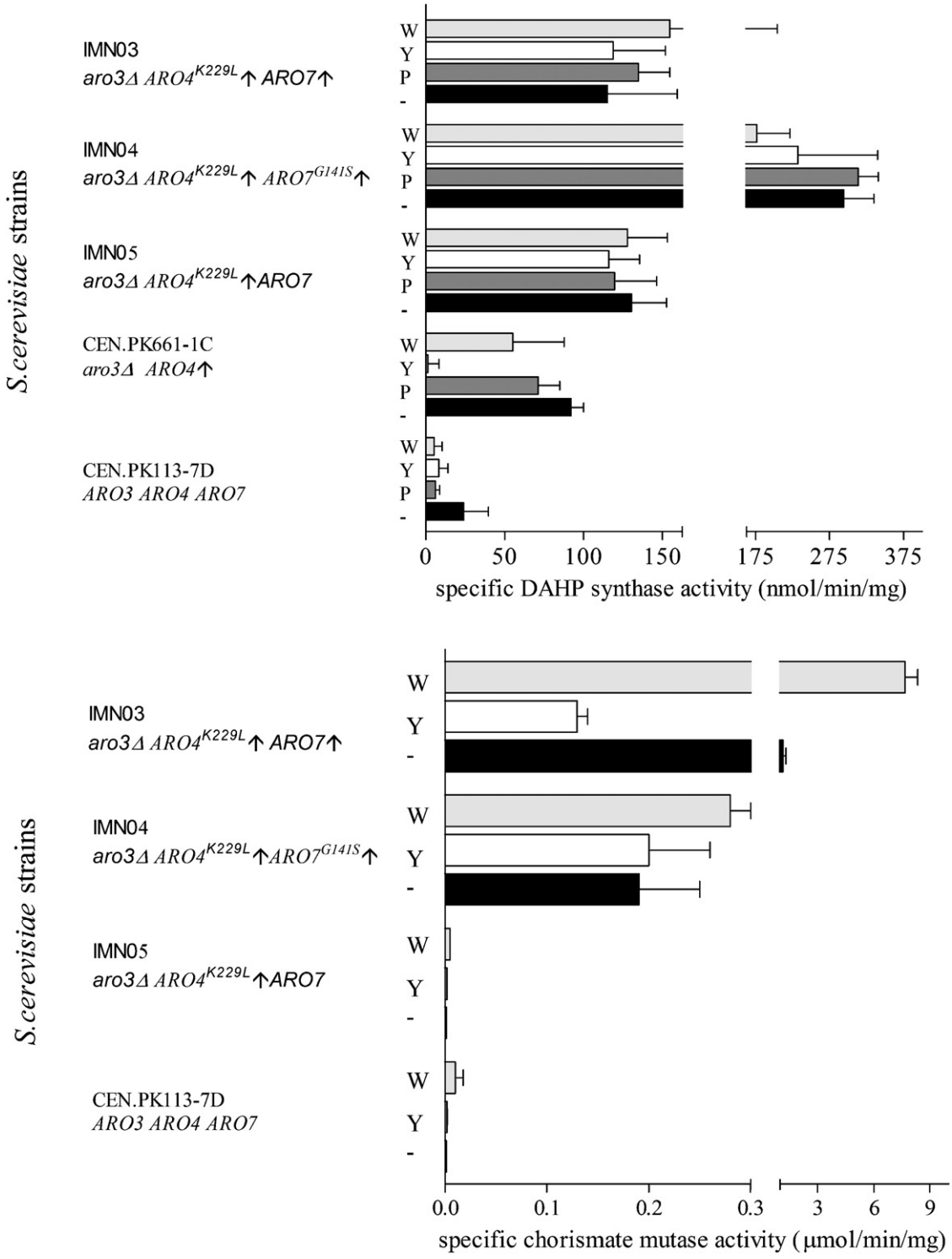

Fig. 3. Activities of DAHP synthase and chorismate mutase in the presence and absence of L-phenylalanine, L-tryptophan and L-tyrosine in the reference *S. cerevisiae* strain CEN.PK113-7D and in strains engineered in key steps of aromatic amino acid biosynthesis. Enzyme activities were assayed in cell extracts of aerobic, glucose-limited chemostat cultures. Data represent the average ± standard deviation of results from two independent chemostat cultures each culture sample being measured in triplicates. ■ Activities without amino acids (−), ▒ activities with 0.5 mM phenylalanine (P), □ activities with 0.5 mM tyrosine (Y), ▨ activities with 0.5 mM tryptophan (W).

they confirmed the complete absence of tyrosine inhibition in the strains carrying the $ARO4^{K229L}$ allele (Fig. 3).

Allosteric control of chorismate mutase was analysed in cell extracts of glucose-limited chemostat cultures. In strains carrying a single chromosomal copy of the wild-type *ARO7* allele, activities of chorismate mutase were close to the detection limit (Fig. 3), which made it difficult to quantify allosteric effects of tyrosine and tryptophan, the two known allosteric regulators of Aro7p (Schmidheini et al., 1989; Schmidheini et al., 1990). Overexpression of the wild-type *ARO7* allele led to an over 50-fold increase of chorismate mutase activities relative to reference strains carrying a single chromosomal copy and confirmed both activation by tryptophan and inhibition by tyrosine (Fig. 3). Finally, overexpression of the $ARO7^{G141S}$ allele led to the complete elimination of both tryptophan activation and tyrosine inhibition (Fig. 3). Although the chorismate mutase activities in strains overexpressing the $ARO7^{G141S}$ allele were lower than those in strains overexpressing the wild-type *ARO7* allele, they were still over 10-fold higher than in strains that carried a single chromosomal copy of *ARO7* (Fig. 3). Plate assays showed that feedback inhibition of Aro7p by tyrosine was less critical than for Aro4p DAHP, as no growth defect was recorded for strains expressing the wild-type *ARO7* allele, IMZ014 and IMZ016. This suggests that the inhibition constant of Aro7p for tyrosine is lower than the K_i reported for Aro4p ($K_i = 0.9\,\mu M$ tyrosine) (Hartmann et al., 2003).

3.2. Tryptophan requirement of strains overexpressing different ARO7 alleles

It has previously been reported that overexpression of *ARO7* leads to tryptophan auxotrophy by preferentially channelling chorismate towards phenylalanine and tyrosine biosynthesis (Krappmann et al., 2000). Although CEN.PK strains that overexpressed the wild-type *ARO7* allele (strains IMZ016, IMZ014, Table 1) exhibited a reduced specific growth rate in shake flask cultures, this could not be restored by tryptophan addition (Table 2). Strains overexpressing the tryptophan-insensitive allele $ARO7^{G141S}$ (IMZ017, IMZ018) (Schnappauf et al., 1998) grew even slower than strains overexpressing the wild-type *ARO7* allele (Table 2). In this case, a partial restoration of growth was observed upon the addition of tryptophan. This partial tryptophan auxotrophy was most pronounced in the strain that expressed both $ARO4^{K229L}$ and $ARO7^{G141S}$ (Table 2). Although the strains carrying the combinatorial overexpression of either *ARO7* or $ARO7^{G141S}$ with $ARO4^{K229L}$ did grow slower than the CEN.PK113-7D reference strain, IMN03, IMN04 and IMN05 did not show any extra tryptophan requirement. The lowest specific growth rate in the absence of tryptophan was $0.15\,h^{-1}$ (strain IMZ018). This enabled us to quantitatively analyse product formation by the engineered strains in chemostat cultures grown at a dilution rate of $0.10\,h^{-1}$ without the need for tryptophan supplementation.

3.3. Analysis of extracellular product formation in chemostat cultures

The impact of the overexpression of the $ARO4^{K229L}$ allele and of the $ARO7^{G141S}$ alleles on biomass yields and on the production of extracellular products was analysed in aerobic, glucose-limited chemostat cultures grown at a dilution rate of $0.10\,h^{-1}$. In all the chemostat cultures, the extracellular concentrations of phenylalanine and tyrosine were below the detection limit of the analysis method ($10\,\mu M$ for both amino acids). However, significant concentrations of the fusel alcohols phenylethanol and *p*-hydroxyphenylethanol, as well as of the corresponding organic acids were detected in several of the cultures (Table 3). Expression of a single copy of the $ARO4^{K229L}$ allele resulted in an over 50-fold increase of the total extracellular concentration of these compounds relative to the isogenic reference strain CEN.PK113-7D, in which concentrations of these compounds were close to or below the detection limit (Table 3). The cloning of the $ARO4^{K229L}$ allele behind the glyceraldehyde-3-phosphate dehydrogenase (*TDH3*) promoter resulted in a 100-fold increase of the extracellular concentration of aromatic compounds (Table 3).

Table 2
Specific growth rate μ (h^{-1}) determination of chorismate-mutase-overexpressing strains mutants in presence and absence of $50\,mg\,l^{-1}$ tryptophan in SM medium with 2% glucose

Strain	Genotype	Maximum specific growth rate μ_{max} (h^{-1})	
		−Trp	+Trp
CEN.PK113-7D	*ARO3 ARO4*	0.39±0.01	0.39±0.01
IMZ016	*ARO3 ARO4 TDH3pr-ARO7*	0.25±0.01	0.26±0.01
IMZ017	*ARO3 ARO4 TDH3pr-*$ARO7^{G141S}$	0.22±0.01	0.27±0.00
IMZ018	*ARO3* $ARO4^{K229L}$ *TDH3pr-*$ARO7^{G141S}$	0.15±0.00	0.35±0.00
IMN03	*aro3Δ TDH3pr::*$ARO4^{K229L}$*TDH3pr::ARO7*	0.33±0.01	0.33±0.01
IMN04	*aro3Δ TDH3pr::*$ARO4^{K229L}$*TDH3pr::*$ARO7^{G141S}$	0.29±0.00	0.29±0.01
IMN05	*aro3Δ ARO7 TDH3pr::*$ARO4^{K229L}$	0.35±0.01	0.34±0.01

Growth rate data are presented as average±mean deviation from three independent shake flask cultures.

Overexpression of both either the wild-type *ARO7* allele or of the *ARO7*^{G141S} had no significant impact on the production of the aromatic fusel alcohols and corresponding acids (Table 3). However, when overexpression of either *ARO7* allele was combined the overexpression of the *ARO4*^{K229L} allele, extracellular concentration of aromatic metabolites increased by over 200-fold relative to the wild-type reference strain, reaching a maximum concentration of 2.8 mM in the strain IMN004 that overexpressed both mutant alleles (Table 3). Besides, the culture supernatants of strains overpressing the *ARO4*^{K229L} allele also exhibited accumulation of shikimate, *p*-hydroxyphenylpyruvate. Moreover, low concentration of chorismate and phenylpyruvate were measured in the strain IMN004 only (Table 4). The relative high level of shikimate and *p*-hydroxyphenylpyruvate (~0.5 mM each) might reflect the presence of rate limiting catalytic steps in the pathway which deduced from the extracellular metabolite profiles might occur at the shikimate kinase and the steps downstream prephenate.

The strains that combined the overexpression constructs for *ARO4*^{K229L}, *ARO7* or *ARO7*^{G141S} all exhibited 5–10% lower biomass yields than the isogenic reference strain CEN.PK113-7D (Table 3). This reduction of the biomass yield was not clearly correlated to the concentrations of aromatic metabolites in the cultures and may therefore reflect an effect of protein burden (Wijker et al., 1995) rather than a specific metabolic effect related to aromatic amino acid metabolism.

3.4. Intracellular amino acid concentrations in chemostat cultures

As the absence of significant extracellular concentrations of aromatic amino acids may reflect a limitation in their export from the cells, intracellular amino acid concentrations were analysed in the reference and engineered strains. The overexpression of the *ARO4*^{K229L} allele led to a 3–4-fold increase of the intracellular concentrations of phenylalanine and tyrosine (Fig. 4). The simultaneous overexpression of the *ARO4*^{K229L} and *ARO7*^{G141S} alleles did not cause a clear further increase of the intracellular phenylalanine and tyrosine concentrations.

Intracellular concentrations of tryptophan were low in the reference strain CEN.PK113-7D (ca. 0.5 mM, Fig. 4).

Table 3
Biomass yields on glucose and extracellular concentrations of fusel alcohols and corresponding organic acids in aerobic, glucose-limited chemostat cultures ($D = 0.10\,h^{-1}$) of different *S. cerevisiae* strains

Strain	Genotype	Biomass yield g (g glucose)$^{-1}$	Phenylethanol (μM)	Phenylacetate (μM)	*p*-Hydroxy-phenylethanol (μM)	*p*-Hydroxy-phenylacetate (μM)	[a]$\sum$ [metabolites]$_{AVG}$ (μM)
CEN.PK113-7D	*ARO3 ARO4*	0.48 ± 0.01	3 ± 0	3 ± 0	< 2	< 2	< 10
CENPK718-5A	*aro3Δ ARO4*^{K229L}	0.46 ± 0.01	220 ± 20	110 ± 10	150 ± 10	17 ± 2	497
IMZ016	*ARO3 ARO4 TDH3pr-ARO7*	0.45 ± 0.02	< 2	< 2	< 2	< 2	< 8
IMZ017	*ARO3 ARO4 TDH3pr-ARO7*^{G141S}	0.44 ± 0.02	< 2	< 2	< 2	< 2	< 8
IMN05	*aro3Δ TDH3pr-ARO4*^{K229L}	0.41 ± 0.01	260 ± 10	500 ± 50	10 ± 1	340 ± 50	1110
IMN04	*aro3Δ TDH3::ARO4*^{K229L}*TDH3pr::ARO7*^{G141S}	0.38 ± 0.00	660 ± 120	1140 ± 160	30 ± 0	940 ± 170	2770
IMN03	*aro3Δ TDH3pr::ARO4*^{K229L}*TDH3pr::ARO7*	0.42 ± 0.00	550 ± 20	950 ± 40	20 ± 10	770 ± 200	2290

Data are presented as average ± mean deviation of results from two independent chemostat cultures for each strain. Each culture sample was measured in triplicates.

[a]Corresponds to the sum of the phenylethanol, phenylacetate, *p*-hydroxyphenylethanol and *p*-hydroxyphenylacetate concentration measured in each culture.

Table 4
Extracellular concentrations of metabolite intermediates of the aromatic amino acid biosynthesis pathway in aerobic, glucose-limited chemostat cultures ($D = 0.10\,h^{-1}$) of different *S. cerevisiae* strains

Strain	Genotype	Shikimate (μM)	Chorismate (μM)	Phenylpyruvate (μM)	p-Hydroxy-phenylpyruvate (μM)	3-dehydro-shikimate (μM)
CEN.PK 113-7D	*ARO3 ARO4*	< 2	< 2	< 2	< 2	< 2
CENPK718-5A	*aro3Δ ARO4*^{K229L}	ND[a]	ND	ND	ND	ND
IMZ016	*ARO3 ARO4 TDH3pr-ARO7*	< 2	< 2	< 2	< 2	< 2
IMZ017	*ARO3 ARO4 TDH3pr-ARO7*^{G141S}	< 2	< 2	< 2	< 2	< 2
IMN005	*aro3Δ TDH3pr-ARO4*^{K229L}	220 ± 20	< 2	10 ± 10	40 ± 10	< 2
IMN004	*aro3Δ TDH3::ARO4*^{K229L}*TDH3pr::ARO7*^{G141S}	690 ± 10	10 ± 2	20 ± 2	470 ± 49	< 2
IMN003	*aro3Δ TDH3pr::ARO4*^{K229L}*TDH3pr::ARO7*	560 ± 190	< 2	< 2	90 ± 40	< 2

Data are presented as average ± mean deviation of results from two independent chemostat cultures for each strain. Each culture sample was measured in triplicates.

[a]Not determined.

Elimination of feedback inhibition on DAHP synthase caused a ca. three-fold increase of the intracellular tryptophan concentration. But once combined with either overexpression of the tryptophan- and tyrosine-insensitive chorismate mutase (encoded by $ARO7^{G141S}$) or with a overexpression of the wild-type *ARO7* allele, the intracellular level of tryptophan dropped to a level even lower than in the CENPK113-7D strain.

The effects of the overexpression of the $ARO4^{K229L}$ and $ARO7^{G141S}$ alleles on intracellular amino acids were not confined to the aromatic amino acids (Fig. 4). Based on their intracellular concentration profiles, two classes of non-aromatic amino acids could be identified. A first group of amino acids did not show a clear correlation with the genotype of the strains and included valine, alanine, glycine, leucine, serine, glutamate, isoleucine and proline (Fig. 4). Concentration changes between the different strains were below 50% for this group of 'non-responsive' amino acids. Interestingly, a second class of amino acids was responsive to the genotype of the strains. This class included glutamine, aspartate, histidine, ornithine, threonine, lysine and methionine, which consistently showed a genotype-dependent concentration profile that closely mirrored that of phenylalanine and tyrosine (Fig. 4). This result demonstrates that deregulation of the amino acid biosynthesis pathway has more widespread repercussions on amino acid biosynthesis.

3.5. Quantification of metabolic fluxes through the phenylalanine–tyrosine branch of aromatic amino acid biosynthesis

In order to quantify the overall effect of the overexpression of the $ARO4^{K229L}$ and $ARO7^{G141S}$ alleles on the metabolic fluxes through the phenylalanine–tyrosine branch of amino acids (i.e. excluding the flux towards tryptophan and related metabolites), three components need to be taken into account:

(i) The specific production rates of the aromatic metabolites phenylethanol, phenylacetate and their *p*-hydroxy derivatives. In calculating the specific production rates mentioned in Table 5, it was assumed that these metabolites do not accumulate inside the cells.

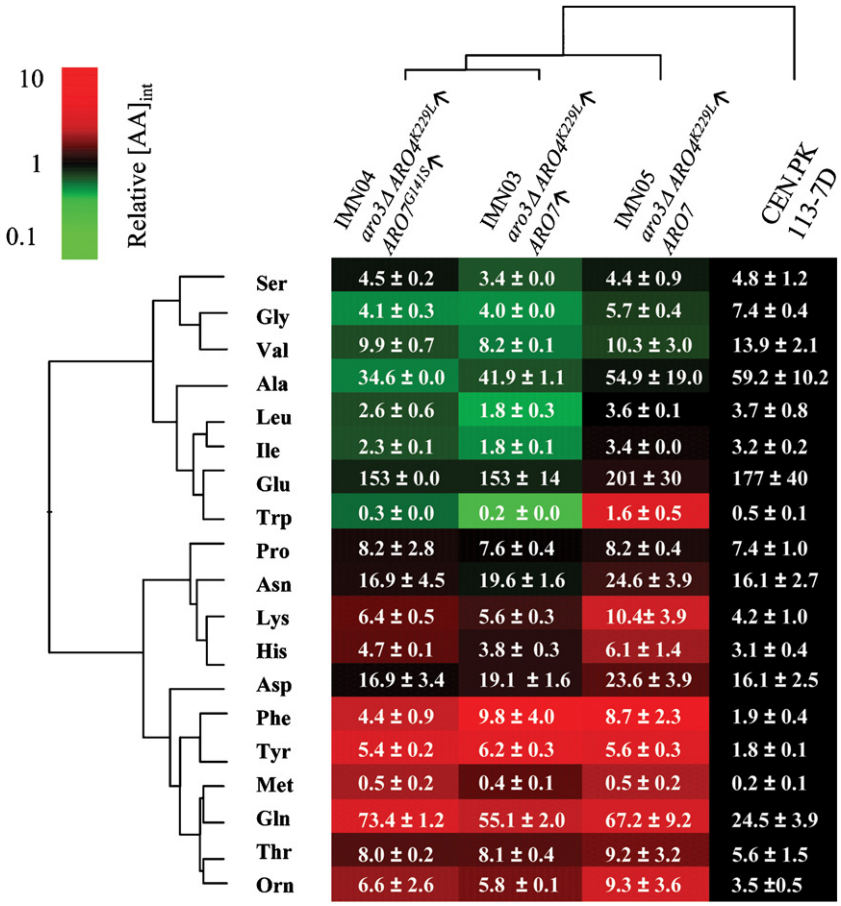

Fig. 4. Intracellular amino acid concentrations in the reference *S. cerevisiae* strain CEN.PK113-7D and in strains engineered in key steps of aromatic amino acid biosynthesis. Numbers indicated the average ± mean deviation of results from two independent chemostat cultures each culture sample being measured in triplicates. Colours represent a concentration heat map normalized for the concentration of each amino acid in cultures of the reference strain CEN.PK113-7D.

Table 5
Specific fluxes through the aromatic amino acid biosynthesis pathway after the chorismate branch

Strain	Genotype	Fluxes (mmol $g^{-1} h^{-1}$)				Normalized flux %
		Aromatic metabolites[a]	Phe and Tyr in protein[b]	Phe and Tyr intracellular[c]	Total	
CEN.PK113-7D	*ARO3 ARO4*	<0.001	0.024	0.043	0.067	100
IMN03	*aro3Δ TDH3p::ARO4^{K229L}TDH3pr::ARO7*	0.092	0.024	0.211	0.327	488
IMN04	*aro3Δ TDH3::ARO4^{K229L}TDH3pr::ARO7^{G141S}*	0.122	0.024	0.143	0.289	431
IMN05	*aro3Δ ARO7 TDH3pr-ARO4^{K229L}*	0.044	0.024	0.198	0.266	397

Total fluxes were calculated by combining (i) specific rates of production of aromatic metabolites (fusel alcohols and acids) derived from phenylalanine and tyrosine, (ii) specific rates of production of phenylalanine and tyrosine in cellular protein and (iii) specific rates of production of intracellular free phenylalanine and tyrosine.

[a]Sum of the phenylethanol, phenylacetate, *p*-hydroxyphenylethanol and *p*-hydroxyphenylacetate concentrations measured multiplied by the dilution rate and divided by the biomass concentration in each culture.

[b]Concentrations of phenylalanine and tyrosine in protein were calculated from published data on protein content and amino acid composition of *S. cerevisiae* (Oura, 1972), multiplied the dilution rate and divided by the biomass concentration in each culture.

[c]Sum of the free intracellular phenylalanine and tyrosine concentrations in the cultures were calculated based on an intracellular volume of 2 ml g biomass^{-1} (Lange and Heijnen, 2001), multiplied by the dilution rate and divided by the biomass concentration in each culture.

(ii) The specific production rate of phenylalanine and tyrosine incorporated into cellular protein. Based on the assumption that the protein content in all strains is identical to that of the reference strain CEN.PK113-7D grown at a dilution rate of 0.10 h^{-1} (Lange and Heijnen, 2001) and that the amino acid composition of the cellular protein is equal to that reported by Oura (1972), this rate is identical for all strains (Table 5).

(iii) The specific production rates of free intracellular phenylalanine and tyrosine, which can be calculated from the data presented in Fig. 4 by assuming an intracellular volume of 2 ml (g biomass)$^{-1}$ (Table 5).

In the reference strain CEN.PK113-7D, the flux towards phenylalanine and tyrosine was virtually completely incorporated into cellular protein. In the strains that overexpressed the *ARO4^{K229L}* allele, the overall flux through this branch of aromatic amino acid metabolism increased by four to five-fold (Table 5). This was primarily due to the increased synthesis of the fusel alcohols and corresponding acids. The increased concentrations of free intracellular phenylalanine and tyrosine had little impact on the overall fluxes.

4. Discussion

This study presents a quantitative analysis of the impact of allosteric control of two key enzymes in aromatic amino acid metabolism on product formation by *S. cerevisiae*. The results demonstrate that DAHP synthase exerts a strong degree of control on the synthesis of aromatic compounds by *S. cerevisiae*. This result is consistent with an earlier report that non-defined feedback insensitive mutants of *S. cerevisiae* obtained by ethyl methyl-sulfonate mutagenesis and screening on phenylalanine analogues produced increased levels of phenylethanol (Fukuda et al., 1991a; Fukuda et al., 1991b). Moreover, elimination of feedback regulation is a classical first step in improving amino acid production by prokaryotes. In contrast with the situation in bacteria such as *E. coli* and *C. glutamicum* (Li et al., 1999; Liao et al., 2001; Baez-Viveros et al., 2004; Sprenger, 2007), the alleviation of feedback inhibition on *S. cerevisiae* DAHP synthase did not lead to measurable extracellular concentrations of phenylalanine or tyrosine. Apparently, even when the intracellular concentration of phenylalanine reached levels of over 60 mM (Fig. 4), export across the plasma membrane did not occur. So far the only system reported to catalyse the export of amino acids from *S. cerevisiae* cells involved the *AQR1* gene product (Velasco et al., 2004), which mediates the export of several amino acids via an exocytosis-like mechanisms. However, phenylalanine and tyrosine are not among the reported substrates for this export system. If *S. cerevisiae* is ever to be considered for the production of amino acids, engineering of product export is clearly a priority target. The steep gradient of phenylalanine that exists across the plasma membrane of *S. cerevisiae* strains that express the *ARO4^{K229L}* and *ARO7^{G141S}* alleles make them ideally suited as a model system to explore strategies for introducing amino acid export into *S. cerevisiae*.

In *S. cerevisiae*, chorismate mutase (Aro7p) is known to be subject to allosteric regulation by tyrosine (inhibition) and tryptophan (activation). Our hypothesis that, especially in strains expressing a feedback insensitive DAHP synthase, this allosteric regulation would have a strong effect on aromatic amino acid biosynthesis was not borne out by the experimental results. In fact, the product concentrations and specific aromatic product formation rates observed in strains with a combined expression of the feedback insensitive *ARO4^{K229L}* and the non-allosterically controlled *ARO7^{G141S}* alleles showed only small differences in the formation of intracellular and extracellular aromatic

products (Fig. 4, Table 2). This indicates that, in strains with a deregulated DAHP synthase, control of the synthesis of aromatic compounds resides elsewhere. However, profiling of extracellular metabolites in strains with a deregulated DAHP synthase revealed the accumulation of intermediates like in particular shikimate and *p*-hydroxyphenylpyruvate pointing out at shikimate kinase and steps downstream prephenate as potential metabolic bottlenecks. It has been shown in *E.coli* that overexpression of several genes involved in the shikimate pathway based on intracellular concentrations have been an efficient method to remove metabolic bottlenecks (Oldigues et al., 2004; Sprenger, 2007). Interestingly, shikimate kinase has been proposed to be one of the major limiting step (Lütke-Eversloh et al., 2007). In contrast to what is known in bacterial systems, no information is available on the allosteric regulation of yeast prephenate dehydrogenase and dehydratase encoded by *TYR1* and *PHA2*, respectively.

Since we have not analysed levels of all intermediates of the aromatic amino acid biosynthesis pathway, a discussion on the actual rate-controlling step(s) in these strains is by necessity speculative. Still, some possibilities may be of special interest in further work.

Firstly in the strains that express the $ARO4^{K229L}$ allele the activity of DHAP synthase may exert a high degree of flux control. In that case, overexpression of $ARO4^{K229L}$ might lead to increased fluxes toward 'fusel' aromatic metabolites (Table 3). Secondly, a systematic overexpression of the genes encoding steps in the aromatic amino acid pathway in combination with the overexpression of the $ARO4^{K229L}$ allele, as performed in *E.coli* or *Corynebacteria* (Oldigues et al., 2004) should help to identify additional bottlenecks. Thirdly, formation of fusel compounds requires the conversion of phenylpyruvate and *p*-hydroxylphenylpyruvate, the penultimate compounds in phenylalanine and tyrosine biosynthesis, respectively, by a TPP-dependent decarboxylase activity (Dickinson et al., 2003; Vuralhan et al., 2003, 2005). Measurements of the activity of this decarboxylase activity in cell extracts of the chemostat cultures of the wild-type and engineered strains yielded only very low activities of this key enzyme activity. We are currently attempting to overexpress phenylpyruvate decarboxylase in *S. cerevisiae*. However, these studies are complicated by the fact that the molecular nature of this decarboxylase activity is not yet fully understood (Vuralhan et al., 2005). Final possibility involves a reaction outside the main pathway for synthesis of aromatic amino acids. The pentose phosphate pathway is essential for aromatic amino acid biosynthesis as it provides E-4P, an essential precursor for the shikimate pathway (Fig. 1). It has been demonstrated that transketolase, the enzyme that catalyses E-4P formation, is inhibited by *p*-hydroxyphenylpyruvate, the penultimate intermediate in tyrosine biosynthesis (Solovjeva and Kochetov, 1999). Although no *p*-hydroxyphenylpyruvate-insensitive mutant forms of yeast transketolase have been described, it may be of interest to exchange the yeast *TKL1*/*TKL2* genes for a heterologous transketolase gene.

The deregulation of the aromatic amino acid biosynthesis pathway had a strong impact on the intracellular concentrations of several non-aromatic amino acids (Fig. 4). We are not aware of regulatory networks that might account for the observation that intracellular concentrations of glutamine, histidine, ornithine, threonine, lysine and methionine all showed genotype-dependent concentration profiles similar to those of phenylalanine and tyrosine (Fig. 4). Involvement of transaminases with overlapping substrate specificities in the synthesis of these amino acids may contribute to this phenomenon by connecting a number of intracellular amino acid—2-oxo acid equilibrium reactions. For example, it is known that the aromatic amino transferase encoded by *ARO8* can also transaminate methionine (Iraqui et al., 1998; Urrestarazu et al., 1998). However, a complete overview of the substrate specificities of the *S. cerevisiae* transaminases is currently not available. The perturbance of non-aromatic amino acid biosynthesis pathways upon the deregulation of the shikimate pathway represents an important challenge for further research on metabolic engineering of aromatic metabolism in *S. cerevisiae*.

Acknowledgments

This work was financially supported by the Dutch government (CW-NWO program "Transition towards Sustainable Technology") and the Kluyver Centre for Genomics of Industrial Fermentation which is supported by The Netherlands Genomics Initiative. Z.V. was financially supported by DSM. We thank Pascale Daran-Lapujade and the DSM discussion group for helpful comments on the manuscript. We thank Dr. P. Kötter (Institüt für Mikrobiologie der J. W. Goethe Universität, Frankfurt, Germany) for providing mutant strains. We thank A. ten Pierick for her technical assistance for measuring intracellular amino acid levels. G. H. B. was supported by the Deutsche Forschungsgemeinschaft.

Appendix. Supplementary materials

Supplementary data associated with this article can be found in the online version at doi:10.1016/j.ymben.2008.02.002.

References

Baez-Viveros, J.L., Osuna, J., Hernandez-Chavez, G., Soberon, X., Bolivar, F., Gosset, G., 2004. Metabolic engineering and protein directed evolution increase the yield of L-phenylalanine synthesized from glucose in *Escherichia coli*. Biotechnol. Bioeng. 87, 516–524.

Ball, S.G., Wickner, R.B., Cottarel, G., Schaus, M., Tirtiaux, C., 1986. Molecular cloning and characterization of *ARO7-OSM2*, a single yeast gene necessary for chorismate mutase activity and growth in hypertonic medium. Mol. Gen. Genet. 205, 326–330.

Brown, J.F., Dawes, I.W., 1990. Regulation of chorismate mutase in *Saccharomyces cerevisiae*. Mol. Gen. Genet. 220, 283–288.

Dickinson, J.R., Salgado, L.E., Hewlins, M.J., 2003. The catabolism of amino acids to long chain and complex alcohols in *Saccharomyces cerevisiae*. J. Biol. Chem. 278, 8028–8034.

Ehrlich, F., 1907. Uber die Bedingungen der Fuselölbildung and über ihren Zusammenhang mit dem Eiweissaufbau der Hefe. Ber. Deut. Chem. Gesellsch. 40, 1027–1047.

Etschmann, M.M., Bluemke, W., Sell, D., Schrader, J., 2002. Biotechnological production of 2-phenylethanol. Appl. Microbiol. Biotechnol. 59, 1–8.

Fabre, C.E., Blanc, P.J., Goma, G., 1998. Production of 2-phenylethyl alcohol by *Kluyveromyces marxianus*. Biotechnol. Prog. 14, 270–274.

Fukuda, K., Watanabe, M., Asano, K., Ouchi, K., Takasawa, S., 1991a. A mutated *ARO4* gene for feedback-resistant DAHP synthase which causes both o-fluoro-DL-phenylalanine resistance and beta-phenethyl-alcohol overproduction in *Saccharomyces cerevisiae*. Curr. Genet. 20, 453–456.

Fukuda, K., Watanabe, M., Asano, K., Ouchi, K., Takasawa, S., 1991b. Isolation and genetic study of *p*-fluoro-DL-phenylalanine-resistant mutants overproducing beta-phenethyl-alcohol in *Saccharomyces cerevisiae*. Curr. Genet. 20, 449–452.

Gietz, R.D., Schiestl, R.H., 2007. High-efficiency yeast transformation using the LiAc/SS carrier DNA/PEG method. Nat. Protoc. 2, 31–34.

Guldener, U., Heck, S., Fielder, T., Beinhauer, J., Hegemann, J.H., 1996. A new efficient gene disruption cassette for repeated use in budding yeast. Nucleic Acids Res. 24, 2519–2524.

Gunby, P., 1983. FDA approves aspartame as soft-drink sweetener. J Am Med Assoc 250, 872–873.

Hartmann, M., Schneider, T.R., Pfeil, A., Heinrich, G., Lipscomb, W.N., Braus, G.H., 2003. Evolution of feedback-inhibited beta /alpha barrel isoenzymes by gene duplication and a single mutation. Proc. Natl. Acad. Sci. USA 100, 862–867.

Helmstaedt, K., Krappmann, S., Braus, G.H., 2001. Allosteric regulation of catalytic activity: *Escherichia coli* aspartate transcarbamoylase versus yeast chorismate mutase. Microbiol. Mol. Biol. Rev. 65, 404–421 table.

Helmstaedt, K., Strittmatter, A., Lipscomb, W.N., Braus, G.H., 2005. Evolution of 3-deoxy-D-arabino-heptulosonate-7-phosphate synthase-encoding genes in the yeast *Saccharomyces cerevisiae*. Proc. Natl. Acad. Sci. USA 102, 9784–9789.

Hermann, T., 2003. Industrial production of amino acids by coryneform bacteria. J. Biotechnol. 104, 155–172.

Ikeda, M., 2003. Amino acid production processes. Adv. Biochem. Eng. Biotechnol. 79, 1–35.

Ikeda, M., Katsumata, R., 1992. Metabolic engineering to produce tyrosine or phenylalanine in a tryptophan-producing *Corynebacterium glutamicum* Strain. Appl. Environ. Microbiol. 58, 781–785.

Iraqui, I., Vissers, S., Cartiaux, M., Urrestarazu, A., 1998. Characterisation of *Saccharomyces cerevisiae ARO8* and *ARO9* genes encoding aromatic aminotransferases I and II reveals a new aminotransferase subfamily. Mol. Gen. Genet. 257, 238–248.

Janke, C., Magiera, M.M., Rathfelder, N., Taxis, C., Reber, S., Maekawa, H., Moreno-Borchat, A., Doenges, G., Schwob, E., Schiebel, E., Knop, M., 2004. A versatile toolbox for PCR-based tagging of yeast genes: fluorescent proteins, more markers and promoter substitution cassettes. Yeast 21, 947–962.

Krappmann, S., Lipscomb, W.N., Braus, G.H., 2000. Coevolution of transcriptional and allosteric regulation at the chorismate metabolic branch point of *Saccharomyces cerevisiae*. Proc. Natl. Acad. Sci. USA 97, 13585–13590.

Kunzler, M., Paravicini, G., Egli, C.M., Irniger, S., Braus, G.H., 1992. Cloning, primary structure and regulation of the *ARO4* gene, encoding the tyrosine-inhibited 3-deoxy-D-arabino-heptulosonate-7-phosphate synthase from *Saccharomyces cerevisiae*. Gene 113, 67–74.

Lange, H.C., Heijnen, J.J., 2001. Statistical reconciliation of the elemental and molecular biomass composition of *Saccharomyces cerevisiae*. Biotechnol. Bioeng. 75, 334–344.

Li, K., Mikola, M.R., Draths, K.M., Worden, R.M., Frost, J.W., 1999. Fed-batch fermentor synthesis of 3-dehydroshikimic acid using recombinant *Escherichia coli*. Biotechnol. Bioeng. 64, 61–73.

Liao, H.F., Lin, L.L., Chien, H.R., Hsu, W.H., 2001. Serine 187 is a crucial residue for allosteric regulation of *Corynebacterium glutamicum* 3-deoxy-D-arabino-heptulosonate-7-phosphate synthase. FEMS Microbiol. Lett. 194, 59–64.

Lowry, O.H., Rosebrough, N.J., Farr, A.L., Randall, R.J., 1951. Protein measurement with the Folin phenol reagent. J. Biol. Chem. 193, 265–275.

Lütke-Eversloh, T., Santos, C.N., Stephanopoulos, G., 2007. Perspectives of biotechnological production of L-tyrosine and its applications. Appl. Microbiol. Biotechnol. 77, 751–762.

Luttik, M.A., Overkamp, K.M., Kotter, P., de Vries, S., van Dijken, J.P., Pronk, J.T., 1998. The *Saccharomyces cerevisiae NDE1* and *NDE2* genes encode separate mitochondrial NADH dehydrogenases catalyzing the oxidation of cytosolic NADH. J. Biol. Chem. 273, 24529–24534.

Mumberg, D., Muller, R., Funk, M., 1995. Yeast vectors for the controlled expression of heterologous proteins in different genetic backgrounds. Gene 156, 119–122.

Oldigues, M., Kunze, M., Degenring, D., Sprenger, G.A., Takors, R., 2004. Stimulation, monitoring, and analysis of pathway dynamics by metabolic profiling in the aromatic amino acid pathway. Biotechnol. Prog. 20, 1623–1633.

Oura, E., 1972. The effect of aeration on the growth energetics and biochemical composition of baker's yeast. Ph.D. Thesis, University of Helsinki, Finland.

Pittard, A.J., 1996. Biosynthesis of aromatic amino acids. In: Neidhardt, F.C., Curtis, III, R., Ingraham, J.L., Lin, E.C.C., Low, K.B., Magasanik, B., Rexnikoff, W.S., Riley, M., Schaechter, M., Umbarger, H.E. (Eds.), *Escherichia coli* and *Salmonella*, Cellular and Molecular Biology. American Society of Microbiology, Washington, DC, pp. 458–484.

Postma, E., Verduyn, C., Scheffers, W.A., van Dijken, J.P., 1989. Enzymic analysis of the crabtree effect in glucose-limited chemostat cultures of *Saccharomyces cerevisiae*. Appl. Environ. Microbiol. 55, 468–477.

Schmidheini, T., Sperisen, P., Paravicini, G., Hutter, R., Braus, G., 1989. A single point mutation results in a constitutively activated and feedback-resistant chorismate mutase of *Saccharomyces cerevisiae*. J. Bacteriol. 171, 1245–1253.

Schmidheini, T., Mosch, H.U., Evans, J.N., Braus, G., 1990. Yeast allosteric chorismate mutase is locked in the activated state by a single amino acid substitution. Biochemistry 29, 3660–3668.

Schnappauf, G., Krappmann, S., Braus, G.H., 1998. Tyrosine and tryptophan act through the same binding site at the dimer interface of yeast chorismate mutase. J. Biol. Chem. 273, 17012–17017.

Solovjeva, O.N., Kochetov, G.A., 1999. Inhibition of transketolase by *p*-hydroxyphenylpyruvate. FEBS Lett. 462, 246–248.

Sprenger, G.A., 2007. From scratch to value: engineering *Escherichia coli* wild type cells to the production of L-phenylalanine and other fine chemicals derived from chorismate. Appl. Microbiol. Biotechnol. 75, 739–749.

Sprinson, D., Srinivasan, P.R., Katagiri, M., 1962. 3-deoxy-D-arabino-hepturosonate-7-phosphate synthetase from *E.coli*. Methods Enzymol. 5, 394–398.

Teshiba, S., Furter, R., Niederberger, P., Braus, G., Paravicini, G., Hutter, R., 1986. Cloning of the *ARO3* gene of *Saccharomyces cerevisiae* and its regulation. Mol. Gen. Genet. 205, 353–357.

Urrestarazu, A., Vissers, S., Iraqui, I., Grenson, M., 1998. Phenylalanine- and tyrosine-auxotrophic mutants of *Saccharomyces cerevisiae* impaired in transamination. Mol. Gen. Genet. 257, 230–237.

van den Berg, M.A., Jong-Gubbels, P., Kortland, C.J., van Dijken, J.P., Pronk, J.T., Steensma, H.Y., 1996. The two acetyl-coenzyme A synthetases of *Saccharomyces cerevisiae* differ with respect to kinetic properties and transcriptional regulation. J. Biol. Chem. 271, 28953–28959.

van Maris, A.J., Geertman, J.M., Vermeulen, A., Groothuizen, M.K., Winkler, A.A., Piper, M.D., van Dijken, J.P., Pronk, J.T., 2004.

Directed evolution of pyruvate decarboxylase-negative *Saccharomyces cerevisiae*, yielding a C2-independent, glucose-tolerant, and pyruvate-hyperproducing yeast. Appl. Environ. Microbiol. 70, 159–166.

Velasco, I., Tenreiro, S., Calderon, I.L., Andre, B., 2004. *Saccharomyces cerevisiae* Aqr1 is an internal-membrane transporter involved in excretion of amino acids. Eukaryot. Cell 3, 1492–1503.

Verduyn, C., Postma, E., Scheffers, W.A., van Dijken, J.P., 1990. Physiology of *Saccharomyces cerevisiae* in anaerobic glucose-limited chemostat cultures. J. Gen. Microbiol. 136, 395–403.

Vuralhan, Z., Morais, M.A., Tai, S.L., Piper, M.D., Pronk, J.T., 2003. Identification and characterization of phenylpyruvate decarboxylase genes in *Saccharomyces cerevisiae*. Appl. Environ. Microbiol. 69, 4534–4541.

Vuralhan, Z., Luttik, M.A., Tai, S.L., Boer, V.M., Morais, M.A., Schipper, D., Almering, M.J., Kotter, P., Dickinson, J.R., Daran, J.M., Pronk, J.T., 2005. Physiological characterization of the *ARO10*-dependent, broad-substrate-specificity 2-oxo acid decarboxylase activity of *Saccharomyces cerevisiae*. Appl. Environ. Microbiol. 71, 3276–3284.

Wijker, J.E., Jensen, P.R., Snoep, J.L., Vaz, G.A., Guiral, M., Jongsma, A.P., de Waal, A., Hoving, S., van Dooren, S., van der Weijden, C.C., 1995. Energy, control and DNA structure in the living cell. Biophys. Chem. 55, 153–165.

Wittmann, C., Hans, M., Bluemke, W., 2002. Metabolic physiology of aroma-producing *Kluyveromyces marxianus*. Yeast 19, 1351–1363.